EXPERIMENTAL EVALUATION OF GNSS-BASED FREQUENCY SYNCHRONIZATION FOR SAR APPLICATIONS

Eduardo Rodrigues Silva Filho, Marc Rodriguez Cassola

Microwaves and Radar Institute of the German Aerospace Center (DLR)

ABSTRACT

Phase synchronization is a crucial requirement for bistatic and multistatic SAR missions. One possible solution for this problem could be to use the same master oscillator for the radar payload and the GNSS receiver, which could allow the recovery of the oscillator phase noise from the carrier phase measurements. This solution would be cost-effective and straightforward, but its effectiveness depends on whether the GNSS receiver would maintain the spectral purity of the master oscillator internally. We executed zero and short baseline experiments to evaluate this technique with a commercial receiver. Despite some unexpected signatures on the carrier phase single-difference measurements, we achieved frequency synchronization of less than 10 ppm and phase synchronization of less than one degree at the L1 carrier frequency after applying a moving average filter of one second at a 10 Hz sampling rate. The results suggest the feasibility of the GNSS-based phase synchronization concept, but further experiments are necessary to evaluate it thoroughly.

Index Terms— Bistatic radar, multistatic radar, frequency synchronization, phase synchronization, GNSS

1. INTRODUCTION

Bistatic and multistatic SAR systems offer several advantages compared to conventional monostatic systems, such as availability of single-pass interferometric data, reduced development costs and risks, and enhanced performance [1]. However, practical implementation of these systems requires overcoming several technical challenges.

The phase synchronization between the reference radar carriers in the transmitting and receiving platforms using different master oscillators is one of the most critical challenges. Residual phase errors between the platforms may cause defocusing, position and phase errors in the computed image, compromising the use for interferometry and tomography[2].

The TanDEM-X mission achieved phase synchronization within a few degrees by exchanging radar pulses between the two satellites through a direct microwave link [3]. This solution requires additional hardware and adds complexity to the system.

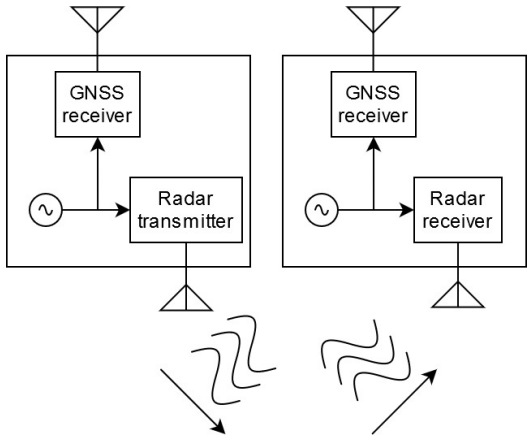

Fig. 1. Evaluated GNSS-based phase synchronization scheme for bistatic and multistatic SAR missions.

In [5] we evaluate through analysis and simulation a GNSS-based phase synchronization technique for multistatic and bistatic systems where in each satellite, the radar payload and the GNSS receiver share the same master oscillator. In this configuration, shown in Fig. 1, the phase difference over time between the oscillators can be recovered from the differential carrier phase measurements after compensating for the relative displacement of the platforms. The technique requires the radar payload and the GNSS receiver to preserve the spectral purity of the reference frequency.

This paper continues the work started in [5] by experimentally demonstrating frequency and phase synchronization through GNSS. Despite not being fully representative of the real case scenario, the results indicate that the setup can estimate frequency differences between two 10 MHz oscillators below mHz level with a commercial receiver. It also suggests that phase synchronization for low radar frequencies can be achieved.

2. GNSS-BASED PHASE SYNCHRONIZATION

Fig. 1 illustrates the evaluated GNSS-based phase synchronization scheme, in which the radar payload and the GNSS receiver share the same oscillator. The oscillator signal is

used within the receiver to generate the reference GNSS signal. At the radar payload, the signal from the oscillator is up-converted to generate the radar carrier.

The frequency offset and phase drift of the master oscillator will reflect directly on the carrier phase measurement. The phase difference between the two signals can be extracted from the carrier phase single differences, which correspond to the difference between the carrier phase measurements for a given tracked GNSS satellite taken by the two receivers at the same epoch. Eq. 1 expresses a biased estimator of the relative phase drifts based on the differential carrier phases measurements for N navigation satellites in view and $n_\lambda^{(i)}$ received GNSS frequencies:

$$\tilde{\psi}_{uv,0} = \frac{2\pi}{\lambda_0} \cdot \sum_{i=1}^{N} \sum_{k=1}^{n_\lambda^{(i)}} \alpha_i \cdot \frac{L_{uv,k}^{(i)} - \tilde{\rho}_{uv}^{(i)}}{n_\lambda^{(i)}}, \qquad (1)$$

where λ_0 is the reference frequency, $L_{uv,k}^{(i)}$ are the differential carrier phase measurements related to frequency k and i-th navigation satellite scaled according to the wavelength and expressed in meters, $\tilde{\rho}_{uv}^{(i)}$ is the difference between the distances from receivers v and u to the i-th navigation satellite, α_i are the weights for the signal from each navigation satellite according to its measured standard deviation. The sum of the weights α_i is equal to one.

This equation will be used in this paper to estimate the phase difference over time for the experiments. The total bias resulting from several uncalibrated delays in this experiment is subtracted from the final result, so only relative synchronization is evaluated in the experiments.

The so-called double difference $L_{uv,k}^{(ij)}$ between measurements from GNSS satellites i and j, for frequency k, is defined as $L_{uv,k}^{(j)} - L_{uv,k}^{(i)}$. Since each single difference contains the relative phase drift signature between the two oscillators, this signature will cancel out in the double difference, leaving only the uncorrelated error sources between the two measurements, mainly determined by the thermal noise. The double difference is used as reference in section 4 to evaluate error components which are correlated between measurements and therefore cannot be reduced by averaging.

3. EXPERIMENT DESCRIPTION

Figs. 2 and 3 illustrate the experiments executed to test phase and frequency synchronization. In both experiments, an Oven Controlled Crystal Oscillator (OCXO) signal is distributed through a splitter to one GNSS receiver and an Arbitrary Waveform Generator (AWS), configured to phase-lock to the external reference. The AWS can introduce frequency and phase offsets to the OCXO signal with high precision. The output of the AWS is used as a frequency reference to the second receiver, and the introduced phase and frequency offsets

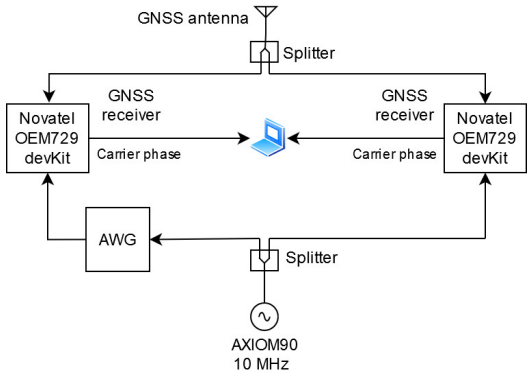

Fig. 2. Zero-baseline phase and frequency synchronization experiment.

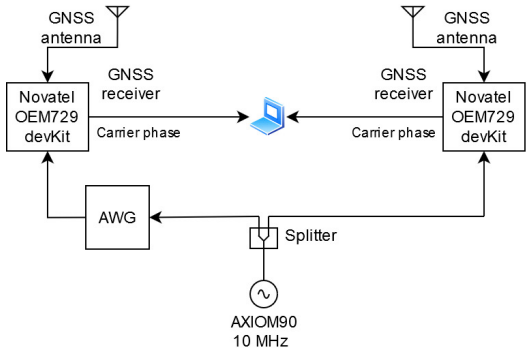

Fig. 3. Short-baseline phase and frequency synchronization experiment.

can be estimated using the technique described in the previous section. We used the OEM729 receiver from Novatel for this experiment.

We executed two variants of the experiment. At the so-called zero-baseline experiment, illustrated in Fig. 2, the GNSS signal received at a single antenna is distributed to the two receivers through a splitter. At the so-called short-baseline experiment, illustrated in Fig. 3, we used two separate antennas positioned approximately one meter apart. We placed the antennas at the rooftop of the Microwaves and Radar Institute of DLR, where there were no considerably higher buildings in the vicinity, which reduces multipath.

In the zero-baseline experiment, most of the external errors cancel out. Therefore it isolates errors generated within the receiver affecting the spectral purity of the reference signal, such as jitter in the frequency synthesis devices. The second experiment includes many additional factors, such as multipath, antenna phase center variations, and local fluctuations on the ionospheric and tropospheric delays. The results obtained from the short baseline can be considered conservative in terms of multipath, signal level, and atmospheric variations compared to space conditions. Therefore its success

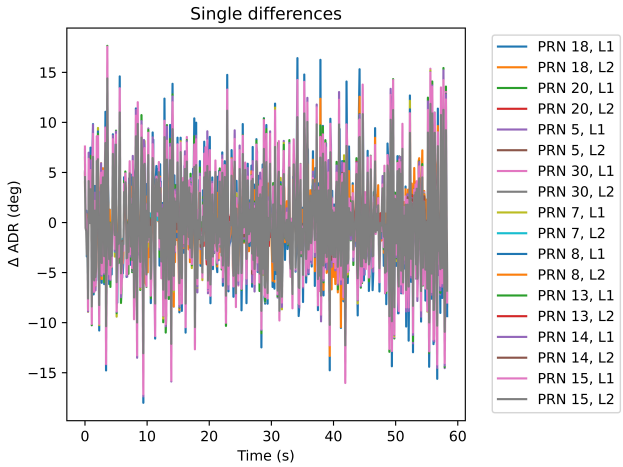

Fig. 4. Single differences results of zero-baseline experiment. The standard deviation of the measurements amounted to 5.9 degrees in average for L1 and 4.7 degrees for L2 signals.

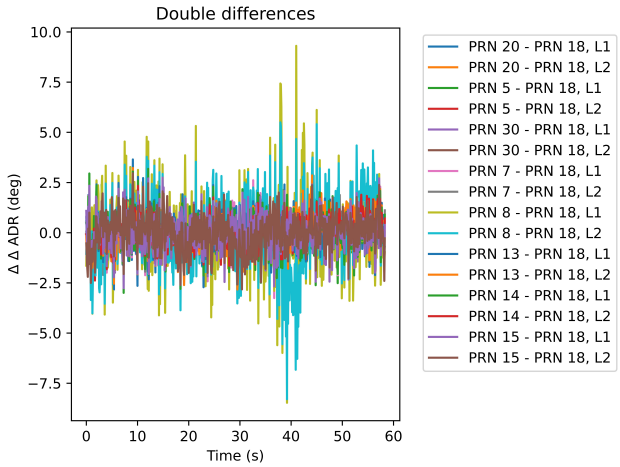

Fig. 5. Double differences results of zero-baseline experiment. The standard deviation of the measurements amounted to 0.9 degrees in average for L1 and 1.1 degrees for L2 signals.

is a strong statement in favor of the technique's feasibility. However, we believe a more elaborate setup is necessary to account for all relevant error sources.

4. RESULTS AND DISCUSSION

Figs. 4 and 5 show the single differences and double differences of the carrier phase measurement for the zero baseline experiment and common oscillator signal. The double-differences correspond to the difference between two single-differences at the same epoch for two tracked GNSS satellites.

We see that the double-differences were within the specified noise level. The single difference presents a higher noise-like signature correlated across different tracked signals. The ratio between the L1 and L2 signatures on the single-differences was approximately the ratio between the corresponding frequencies. This proportionality and the correlation across different tracked signals point to contamination of the reference frequency by the internal receiver electronics, most likely by the frequency synthesis devices. This higher error on the single-differences seems not to be uncommon among receivers that can take external frequency references, since Weinbach et al. mentioned similar findings in [6], where they report results from analogous experiments but with different receivers. The problem, therefore, is likely to be recurring in commercial GNSS receivers to some extent.

Despite the unexpected signatures on the single-differences, the result shown in Fig. 6 indicates that the receivers could be used out-of-the-box for phase synchronization at low radar frequencies. The figure shows the estimated differential phase drifts estimated using Eq. 1, filtered through a moving average with a one-second window. The standard deviation, in this case, was 0.8 degrees in the L-band, which is appropriate for relative phase synchronization.

Fig. 7 demonstrates that the technique can follow phase variations in the reference and that the results are still satisfactory considering multipath and phase center variations, since this was a short-baseline experiment. The standard deviations at each plateau were around 5 degrees, without averaging in time. There was a slow linear drift of the average, which amounted to around 12 degrees total for 210 seconds. The reason for this linear drift is suspected to be an error in compensating the baseline velocity over time, which needs to be further investigated.

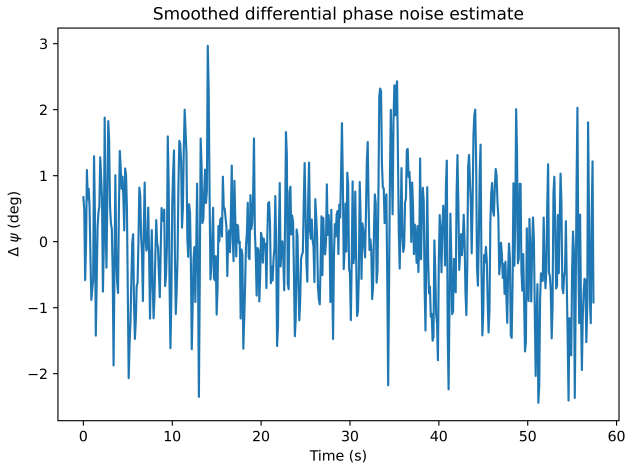

Fig. 6. Estimated phase difference of zero-baseline experiment smoothed with a moving average with 10 sample window at 10 Hz. The standard deviation of the measurements amounted to 0.9 degrees.

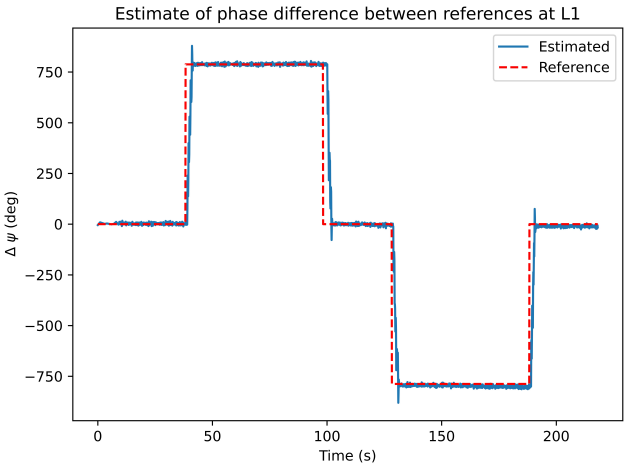

Fig. 7. Phase profile estimation results with short-baseline experiment.

Fig. 8 demonstrates the capability of the technique for frequency synchronization. The frequency was estimated through linear regression of the single differences, scaled to the reference frequency. The estimation of frequency differences with high accuracy is useful in the SAR interferometric processing, which justifies the employment of the technique also for high radar frequency bands such as C-band and X-band. The figure shows the average of the error and the standard deviation. We consider the standard deviation more representative of the performance since the mean error is likely to be mainly caused by a measurement error due to the imprecision of the AWS.

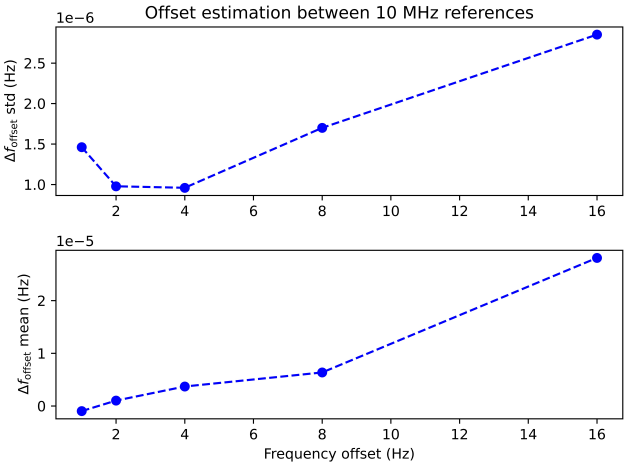

Fig. 8. Frequency estimation results with short-baseline experiment. For each experiment 10 estimations were done based on 1 minute data takes.

5. CONCLUSIONS

The preliminary results indicate that the evaluated GNSS-based phase synchronization technique can achieve good frequency synchronization and sufficient phase synchronization for lower radar frequencies. It shows that the technique could be readily applied for lower frequencies such as L-band and could cover higher frequencies if the receiver keeps the signatures on the single-differences detected in our experiments low, which we believe could be achieved if a receiver is designed for this application. Given the simplicity and effectiveness of the technique, we believe it is bound to become a standard in bistatic and multistatic SAR missions.

6. REFERENCES

[1] G. Krieger and A. Moreira, "Spaceborne bi- and multistatic synthetic aperture radar: potential and challenges," *IEE Proc. Radar Sonar Navig.*, vol. 153, no. 3, pp. 184–198, June 2006.

[2] G. Krieger and M. Younis, "Impact of oscillator noise in bistatic and multistatic SAR," *IEEE Geosci. Remote Sens. Lett.*, vol. 3, no. 3, pp. 424–428, July 2006.

[3] H. Braubach and M. Voelker, "Method for drift compensation with radar measurements with the aid of reference radar signals," April 2007.

[4] Gerhard Krieger, Mariantonietta Zonno, Josef Mittermayer, Alberto Moreira, Sigurd Huber, and Marc Rodriguez-Cassola, "Mirrorsar: A fractionated space transponder concept for the implementation of low-cost multistatic sar missions," in *EUSAR 2018; 12th European Conference on Synthetic Aperture Radar*, Aachen, Germany, June 2018, VDE, pp. 1–6.

[5] Eduardo Rodrigues Silva Filho and Marc Rodriguez Cassola, "Analysis of a pod-based approach for phase and time synchronization of bistatic and multistatic sar systems," in *EUSAR 2021; 13th European Conference on Synthetic Aperture Radar*, Leipzig, Germany, 03 2021, pp. 2147–4403.

[6] U. Weinbach, S. Schon, and T. Feldmann, "Evaluation of state-of-the-art geodetic gps receivers for frequency comparisons," in *2009 IEEE International Frequency Control Symposium Joint with the 22nd European Frequency and Time forum*. 2009, pp. 263–268, IEEE.